LETTERS

Thermochemical structures beneath Africa and the Pacific Ocean

Allen K. McNamara[1]† & Shijie Zhong[1]

Large low-velocity seismic anomalies have been detected in the Earth's lower mantle beneath Africa and the Pacific Ocean that are not easily explained by temperature variations alone[1–11]. The African anomaly has been interpreted to be a northwest–southeast-trending structure[3–5,7] with a sharp-edged linear, ridge-like morphology[9,10]. The Pacific anomaly, on the other hand, appears to be more rounded in shape[1–4,6,7,11]. Mantle models with heterogeneous composition have related these structures to dense thermochemical piles or superplumes[12–19]. It has not been shown, however, that such models can lead to thermochemical structures that satisfy the geometrical constraints, as inferred from seismological observations. Here we present numerical models of thermochemical convection in a three-dimensional spherical geometry using plate velocities inferred for the past 119 million years[20]. We show that Earth's subduction history can lead to thermochemical structures similar in shape to the observed large, lower-mantle velocity anomalies. We find that subduction history tends to focus dense material into a ridge-like pile beneath Africa and a relatively more-rounded pile under the Pacific Ocean, consistent with seismic observations.

Although many geodynamical studies have been performed to better understand the dynamical consequences of a dense layer in the Earth's mantle, only a subset of these have investigated the three-dimensional morphology of such a layer[16–19], and because of technical limitations, these have mainly considered only rectangular cartesian geometries. Cartesian experiments have been very important to our understanding of thermochemical structures in a fluid-dynamical context, but the restrictive box-shape of these experiments has precluded the ability to understand the effects of Earth-like conditions such as spherical geometry and plate-like boundary conditions. As a consequence, the actual shape of thermochemical structures predicted for the Earth could only be roughly inferred from experiments. For example, in laboratory experiments, the sides of the cartesian domain would serve as a proxy for static, circum-Pacific subduction; but this inference does not allow for the more-complicated geometry and time-dependent nature of plate boundaries, and it is also unlikely that this inference would hold for the more complicated subduction patterns associated with the African region.

In previous work with free-slip surface boundary conditions[21], we concentrated on understanding the roles that spherical geometry and rheology play in the formation of thermochemical structures. It was found that temperature-dependent rheology leads to the formation of weak, dense piles that are passively swept aside by cold, downwelling material, resulting in a ubiquitous network of linear ridges of dense material. Only by additionally imposing an unlikely high intrinsic viscosity increase to the dense material can rounded superplumes of dense material form. This work suggested that rounded superplume structures (as proposed for the Pacific) and linear piles (as proposed for Africa) are not expected to be present together within the Earth under the given model parameters. Like previous three-dimensional studies[16–19], these generalized fluid dynamical calculations provided insight into the dynamical character of thermochemical structures in a planet without Earth-like plate tectonics, but without using Earth's plate history, it was not possible to predict two large hot anomalies that could be confidently compared to the seismic anomalies observed beneath Africa and the Pacific.

Here we hypothesize that Earth's plate motion history plays a controlling role in the development of thermochemical structures that geometrically resemble to first order the general shape and locations of the large negative seismic anomalies in the lower mantle. Specifically, we investigate whether the resultant thermochemical structures are consistent with a northwest–southeast (NW–SE)-trending structure beneath Africa that has a ridge-like structure as inferred from raypath studies[9,10], and a more-rounded (less-linear) structure beneath the Pacific. To test this, thermochemical mantle models with initial layer thicknesses of 127 km, 255 km and 956 km for the bottom dense layer are investigated, all having a buoyancy ratio of 0.6 leading to density contrasts of 2–5% (depending upon parameters chosen for the non-dimensionalization factors of temperature and coefficient of thermal expansion). The calculations are carried out for 119 million years of model time and employ surface boundary conditions consistent with 11 stages of plate history[20] as used in similar studies on isochemical convection[22,23]. Unless otherwise noted, initial temperature conditions (at 119 Myr ago) are radial temperature profiles derived from similar two-dimensional axisymmetric thermochemical calculations without plate boundary conditions.

The thermochemical extension[21] of the parallel finite element code CitcomS[24] is used to solve the conservation equations of mass, momentum and energy in the Boussinesq approximation with constant thermodynamic properties. The details, along with formal definitions of the parameters and scalings, are found in previous work[21]. These calculations have much higher resolution than our previous three-dimensional spherical studies, and are performed on a mesh exceeding 3 million elements, divided between 24 processor-computational domains. Over 30 million tracers are used to characterize the compositional field. Improved algorithmic and technical computational abilities allow us to resolve viscosities consistent with Earth-like convective vigour[25], where the Rayleigh number (defined as $\mathrm{Ra} = \alpha g \rho \Delta T h^3 / \kappa \eta_o$) is 2.7×10^8; here α, g, ρ, ΔT, h, κ and η_o are respectively the coefficient of thermal expansion, acceleration of gravity, density, temperature drop across the mantle, mantle depth, thermal diffusivity and upper-mantle reference viscosity. A temperature- and depth-dependent rheology of the non-dimensional form is employed:

$$\eta(T, \mathbf{r}) = \eta_r(z) \exp[A(0.5 - T)]$$

[1]Department of Physics, University of Colorado, Boulder, Colorado 80309-0390, USA. †Present address: Department of Geological Sciences, Arizona State University, Tempe, Arizona 85287, USA.

Here $\eta_r(z) = 1$ for $z < 663$ km and $\eta_r(z) = 0.1225z - 51.2$ for 663 km $\leq z \leq$ 2,867 km, where η and z are the non-dimensional viscosity and dimensional depth, respectively. This formulation leads to a weak upper mantle, a 30 × viscosity step at the upper–lower mantle boundary, and a 10 × linear increase with depth to the base of the mantle. This depth-dependent structure is similar to that used by Bunge *et al.*[22,23], however, these calculations also include temperature-dependent viscosity. A non-dimensional activation coefficient, $A = 9.2103$, is chosen, which leads to a temperature-induced viscosity contrast of 10^4. The models are heated from both below and internally with a non-dimensional heat production of 10. The calculations performed here allow for realistic plate scaling, the advantage being that our diffusion time is consistent with the material transit time. The use of plate velocity boundary conditions guides subduction to occur at locations determined by the plate history. We were careful to employ a convective vigour (Rayleigh number) that is consistent with the plate boundary conditions guiding rather than driving the flow, which minimizes concerns associated with employing kinematic boundary conditions.

Figure 1 shows different perspectives of the three-dimensional compositional fields of the three calculations for a time near the end of the calculation equivalent to the present day. The first two rows show the three-dimensional seismic tomography fields of Ritsema *et al.*[4] and Grand[7] for comparison to the three geodynamical results displayed in the lower three rows. As observed in previous work[17–19,21], dense material is swept into ridges, but for the two lower volume cases (127 km, 255 km), the plate history incorporated here acts to focus and overlap several of these ridges under the Pacific, forming a large, contiguous pile of dense material. In contrast, material is piled into a NW–SE-directed ridge under Africa which curves eastward under Europe. The Pacific anomaly is areally extensive and contains multiple topographic peaks, whereas the African structure is a single-peaked ridge of mid-mantle height. The more-voluminous dense material case (956 km) develops extensive dense piles present everywhere except for areas in the immediate vicinity of subduction regions, and this case would produce anomalies much larger than those observed in tomography.

Temperature fields in both map format and equatorial slices for the final time (present day) of the three calculations with different initial layer thicknesses are shown in Fig. 2a. For comparison, two tomography maps[3–5] are shown at lower-mantle depth slices in Fig. 2b and c. As expected, the pattern of subducted slabs is similar for all three cases in shallower mantle regions. At greater depths, the dense piles of material are easily discerned in the temperature field because of the high degree of heat they retain. The general trend of the piles is similar for all three cases, and in the two thinner layer

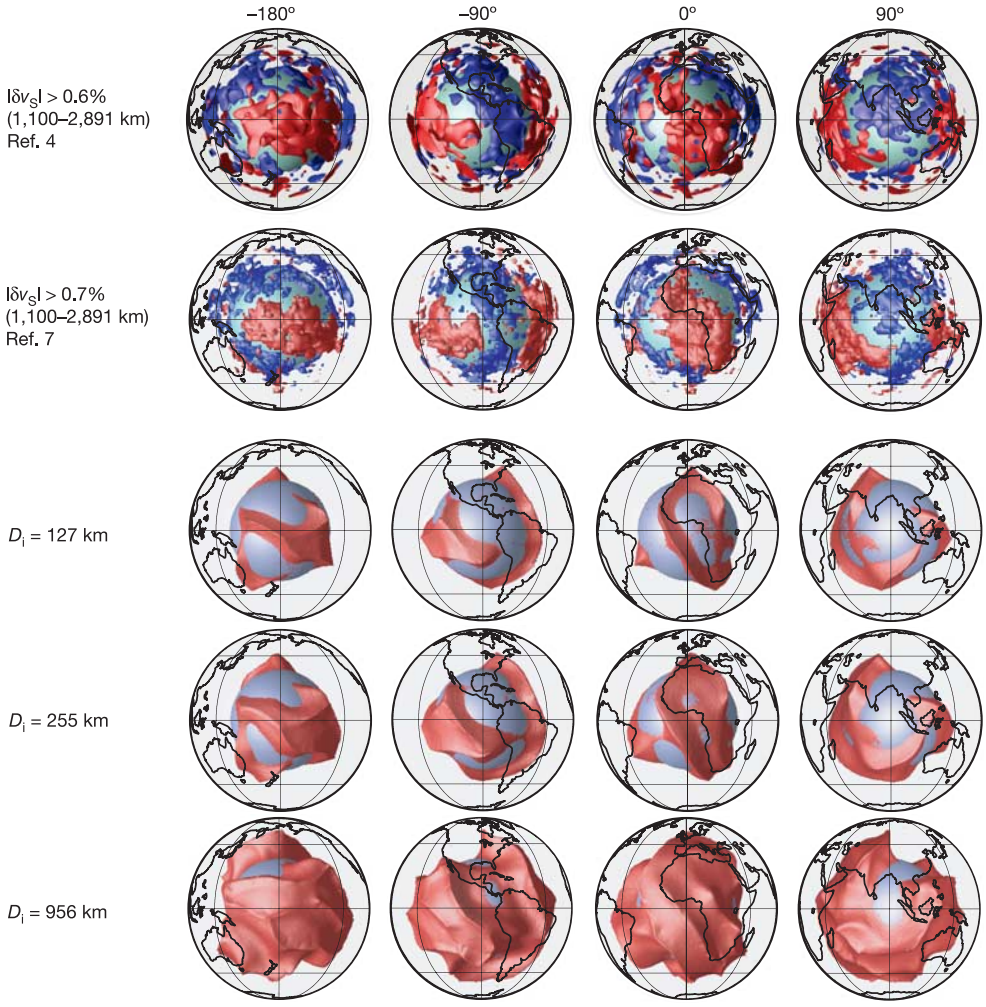

Figure 1 | Perspective views of two tomography models[4,7] and geodynamic compositional fields at the end of the calculations, corresponding to the present day. The four columns represent hemispherical views centred on (left to right) the international dateline, longitude −90°, the prime meridian, and longitude 90°. The tomographic plots display isosurface contours of the shear wave velocity anomaly, δv_S, and do not include data at depths less than 1,100 km to aid in visualization. Blue and red surfaces represent faster and slower than average velocities, respectively. The geodynamic results are from calculations with initial layer thicknesses (D_i) of 127 km, 255 km and 956 km.

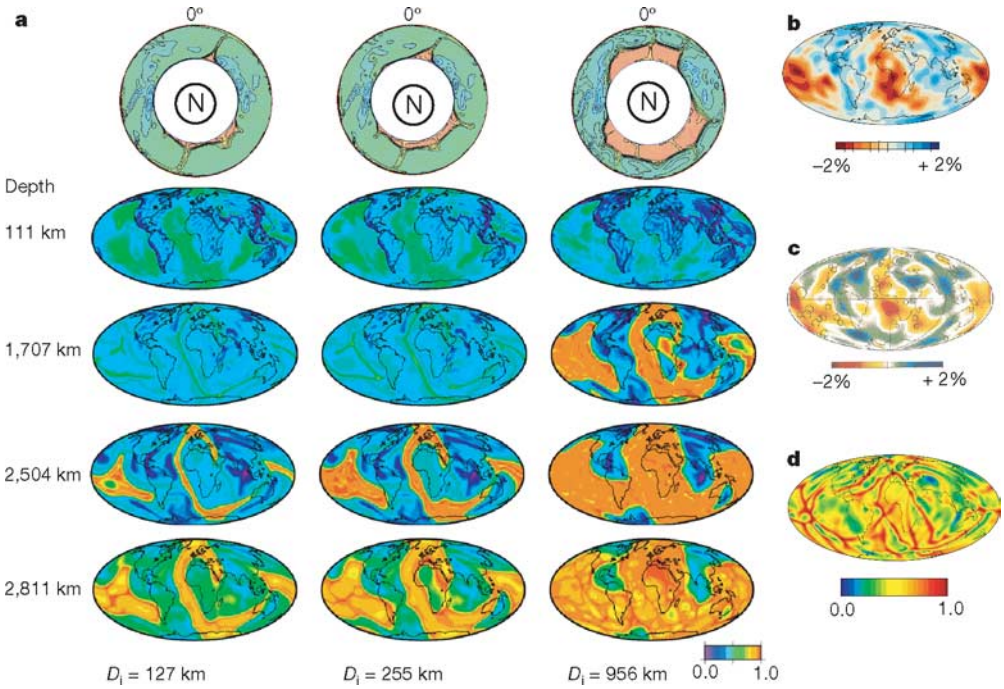

Figure 2 | Temperature and tomography maps. a, Present-day temperature fields for cases with initial dense layer thicknesses of 127 km, 255 km and 956 km (columns). The top row contain equatorial slices (North Pole pointing out of the page, prime meridian at the top). The other rows show temperature slices for 111 km, 1,707 km, 2,504 km and 2,811 km depth. **b**, **c**, Tomography maps at 2,811 km depth[4] (**b**) and the core–mantle boundary[5] (**c**; with hotspots shown as circles) for comparison to the bottom set of geodynamical results in **a**. Temperature map (2,811 km depth) from an isochemical case lacking a dense component. The temperature and tomography maps display non-dimensional temperature and shear wave velocity anomaly, respectively.

cases, there is a NW–SE ridge structure beneath Africa that bends eastward into Europe and the Indian Ocean, not unlike that observed in tomography[1,3,4,7], and an intersection of ridges under the Pacific, resulting in a large continuous pile of dense material there. These thermal maps are strikingly different from those of an identical isochemical calculation (Fig. 2d), which reveal a much smaller-scale and ubiquitous structure of upwellings, similar to previous isochemical studies[23].

It is found that the volume of dense material controls the areal extent and the height of these structures, and the thickest dense layer case does not predict isolated thermochemical structures in the lower mantle. We have discovered from other calculations (not shown here) that decreasing the density contrast leads to decreased areal extent and increased height of the structures, but the general trend of the piles remains unchanged.

The role that initial condition plays in these calculations was also investigated. Whereas the previous cases started with a laterally uniform temperature field, we performed two additional thermochemical cases for the 255-km-thick initial layer case in which the initial 119-Myr-ago plate velocity was maintained for an additional 60 and 120 Myr before starting the time sequence of plate velocity boundary conditions. Present-day results are shown in Fig. 3, and should be compared to the lowermost panel of the 255 km case in Fig. 2. With the new initial conditions, the general trend of a NW–SE ridge beneath Africa and a convergence of ridges beneath the Pacific remains, although the detailed morphology may differ somewhat. More specifically, extending the initial stage of plate motion acts to impose a pre-existing slab structure at the beginning of the calculations which effectively and artificially extends the subduction time related to the Africa–Eurasian convergence, causing excessive amounts of slab material to accumulate beneath present-day Africa. As a result of slow thermal diffusion, this material resides there until the present day, producing a somewhat different morphology.

This work investigates spherical thermochemical convection using a depth- and temperature-dependent viscosity and a realistic plate history as surface boundary conditions. A 'first choice' of Earth-like material parameters has led to a predicted geometry of thermochemical piles that resembles to first order the anomalies observed in seismic tomography. In addition, the sharp NW–SE-trending single-ridged African pile is consistent with that inferred from raypath studies[9,10]. The allowable material parameter space is immense, and because the 'first-choice' parameters produce structures geometrically similar to those observed, we propose that the first-order morphology of a dense component is not overly sensitive to input parameters. We note that uncertainty in geodynamic parameters warrants a much broader future study, and it is not expected that current results would match higher-order geometric features that are seismically observed. Because of the imperfect distribution of seismic sources and receivers, tomography provides a filtered view of actual lower-mantle structures, and we propose that the approach used here combined with tomographic filtering of geodynamic data promises to provide a wealth of previously unavailable material information as

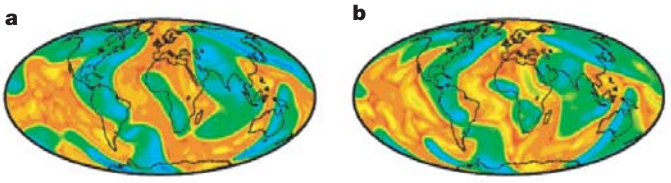

Figure 3 | Effect of initial condition. Temperature fields at 2,811 km depth for thermochemical cases with an initial dense layer thickness of 255 km. The initial stage of plate motion was held fixed for **a**, 60 Myr, and **b**, 120 Myr, before the entire time sequence of plate motion began. These should be compared with the lower panel of the 255 km case in Fig. 2. Colour scale as in Fig. 2a.

more intensive parameter searches are used to more closely relate geodynamic predictions to higher-order seismic results.

Received 13 October 2004; accepted 21 July 2005.

1. Su, W. & Dziewonski, A. M. Simultaneous inversion for 3-D variations in shear and bulk velocity in the mantle. *Phys. Earth Planet. Inter.* **100,** 135–156 (1997).
2. Breger, L. & Romanowicz, B. Three-dimensional structure at the base of the mantle beneath the central Pacific. *Science* **282,** 718–720 (1998).
3. Ritsema, J., van Heijst, H. J. & Woodhouse, J. H. Complex shear wave velocity structure imaged beneath Africa and Iceland. *Science* **286,** 1925–1928 (1999).
4. Ritsema, J., van Heijst, H. J. & Woodhouse, J. H. Global transition zone tomography. *J. Geophys. Res.* **109,** doi:10.1029/2003JB002610 (2004).
5. Kuo, B. Y., Garnero, E. J. & Lay, T. Tomographic inversion of S-SKS times for shear velocity heterogeneity in D″: degree 12 and hybrid models. *J. Geophys. Res.* **105,** 28139–28157 (2000).
6. Masters, G., Laske, G., Bolton, H. & Dziewonski, A. in *Earth's Deep Interior: Mineral Physics and Tomography from the Atomic to the Global Scale* (eds Karato, S. *et al.*) 63–87 (Geophys. Monogr. Ser., Vol. 117, AGU, Washington DC, 2000).
7. Grand, S. P. Mantle shear-wave tomography and the fate of subducted slabs. *Phil. Trans. R. Soc. Lond. A* **360,** 2475–2491 (2002).
8. Wen, L., Silver, P., James, D. & Kuehnel, R. Seismic evidence for a thermo-chemical boundary at the base of the Earth's mantle. *Earth Planet. Sci. Lett.* **189,** 141–153 (2001).
9. Ni, S., Tan, E., Gurnis, M. & Helmberger, D. Sharp sides to the African superplume. *Science* **296,** 1850–1852 (2002).
10. Ni, S. & Helmberger, D. V. Seismological constraints on the South African superplume: Could be the oldest distinct structure on Earth. *Earth Planet. Sci. Lett.* **206,** 119–131 (2003).
11. Ishii, M. & Tromp, J. Constraining large-scale mantle heterogeneity using mantle and inner-core sensitive normal modes. *Phys. Earth Planet. Inter.* **146,** 113–124 (2004).
12. Tackley, P. J. in *The Core-Mantle Boundary Region* (eds Gurnis, M., Wysession, M. E., Knittle, E. & Buffett, B. A.) 231–253 (Geodyn. Ser. Vol. 28, AGU, Washington DC, 1998).
13. Davaille, A. Simultaneous generation of hotspots and superswells by convection in a heterogeneous planetary mantle. *Nature* **402,** 756–760 (1999).
14. Kellogg, L. H., Hager, B. H. & van der Hilst, R. D. Compositional stratification in the deep mantle. *Science* **283,** 1881–1884 (1999).
15. Tackley, P. J. Mantle convection and plate tectonics: toward an integrated physical and chemical theory. *Science* **288,** 2002–2007 (2000).
16. Davaille, A., Girard, F. & Le Bars, M. How to anchor hotspots in a convecting mantle? *Earth Planet. Sci. Lett.* **203,** 621–634 (2002).
17. Jellinek, A. M. & Manga, M. The influence of a chemical boundary layer on the fixity, spacing, and lifetime of mantle plumes. *Nature* **418,** 760–763 (2002).
18. Jellinek, A. M. & Manga, M. Links between long-lived hot spots, mantle plumes, D″, and plate tectonics. *Rev. Geophys.* **42,** doi:10.1029/2003RG000144 (2004).
19. Tackley, P. J. Strong heterogeneity caused by deep mantle layering. *Geochem. Geophys. Geosyst.* **3,** 1024, doi:10.1029/2001GC000167 (2002).
20. Lithgow-Bertelloni, C. & Richards, M. A. The dynamics of Cenozoic and Mesozoic plate motions. *Rev. Geophys.* **36,** 27–78 (1998).
21. McNamara, A. K. & Zhong, S. Thermochemical structures within a spherical mantle: Superplumes or piles? *J. Geophys. Res.* **109,** B07402, doi:10.1029/2003JB002847 (2004).
22. Bunge, H. P. *et al.* Timescales and heterogeneous structure in geodynamic Earth models. *Science* **280,** 91–95 (1998).
23. Bunge, H. P., Richards, M. A. & Baumgardner, J. R. Mantle-circulation models with sequential data assimilation: inferring present-day mantle structure from plate-motion histories. *Phil. Trans. R. Soc. Lond. A* **360,** 2545–2567 (2002).
24. Zhong, S., Zuber, M. T., Moresi, L. & Gurnis, M. Role of temperature-dependent viscosity and surface plates in spherical shell models of mantle convection. *J. Geophys. Res.* **105,** 11063–11082 (2000).
25. Mitrovica, J. X. & Forte, A. M. A new inference of mantle viscosity based upon joint inversion of convection and glacial isostatic adjustment data. *Earth Planet. Sci. Lett.* **225,** 177–189 (2004).

Acknowledgements We thank C. Lithgow-Bertelloni and T. Becker for furnishing us with the plate velocity data used in these calculations. We also thank J. Ritsema and E. Garnero for discussions and for help in generating figures for this manuscript. This work was supported by the David and Lucile Packard Foundation and the National Science Foundation.

Author Information Reprints and permissions information is available at npg.nature.com/reprintsandpermissions. The authors declare no competing financial interests. Correspondence and requests for materials should be addressed to A.K.M. (allen.mcnamara@asu.edu).